ELSEVIER

Journal of Biomechanics 32 (1999) 803–810

JOURNAL OF BIOMECHANICS

www.elsevier.com/locate/jbiomech

Hydrodynamics optimization in butterfly swimming: position, drag coefficient and performance

Redha Taïar[a,*], Pierre Sagnes[b], Claude Henry[c], Anne Béatrice Dufour[a], Annie Hélène Rouard[a]

[a]*Centre de Recherche et d'Innovation sur le Sport, Université Claude Bernard, 27-29 Bd du 11 Novembre 1918, 69622 Villeurbanne Cedex, France*
[b]*Laboratoire d'Ecologie des Eaux Douces et des Grands Fleuves, ESA CNRS 5023, 43 Bd du 11 Novembre 1918, 69622 Villeurbanne Cedex, France*
[c]*Laboratoire de Mécanique des Fluides, Institut National des Sciences Appliquées, 69621 Villeurbanne Cedex, France*

Received 8 March 1999

Abstract

A kinematic study allowed to define the three most propulsive positions during a butterfly swimming cycle, which were: the end of the external sweep, the end of the internal sweep and the end of thrust. These instantaneous positions were different for the ex-world champion Pankratov when compared to another swimmer. Using manikins and a drag-measuring device, we showed that the end of the internal sweep induced the highest drag values and that Pankratov may reduce energy expenditure by taking up a particular position during the end of the swimming cycle. These results point out the relations between swimming movements, passive drag and swimmers' performance.

Keywords: Reynolds number; Drag-measuring device; Kinematic analysis; Propulsive positions; Energy gain

1. Introduction

The drag opposed to a moving submerged body is 500–600 times higher than in the air and is an important force to withstand for swimmers. In this context, their performances not only depend on their own propulsive abilities, but also on their capacities to reduce drag forces to a minimum during swimming. According to the usual formula (Vogel, 1994), the drag force (D, in N) of a swimmer can be calculated as

$$D = \frac{1}{2}\rho S V^2 C_d, \tag{1}$$

Where ρ is the freshwater density (kg m^{-3}), S the frontal surface area (m^2); V the swimming speed (m s^{-1}) and C_d the drag coefficient (dimensionless). In order to facilitate comparisons between different swimmers, we will focus on the study of this C_d, which can easily be calculated from (1) using the following transformation:

$$C_d = \frac{2D}{\rho S V^2}. \tag{2}$$

The C_d depends on the body morphology as well as on the Reynolds number (Re, another dimensionless coefficient). The Re expresses the ratio between inertial forces and viscous forces around a submerged body (i.e., the conditions of the turbulences around this body). Re can be calculated using the following equation:

$$Re = \frac{LV}{v}, \tag{3}$$

Where L is the body length (m) and v the kinematic viscosity of the fluid (m^2 s^{-1}). Theoretically, as Re values increase, C_d values decrease up to a critical value of Re above which C_d values remain stable (Vogel, 1994). At a given Re, the smaller the C_d of a body is the more hydrodynamic it is and C_d differences between two bodies at high Re are mainly due to shape differences.

* Corresponding author. Tel.: 00-33-04-72-43-10-91; fax: 00-33-04-72-44-80-27.
E-mail address: taiar@univ-lyon1.fr (R. Taïar)

0021-9290/99/$ - see front matter
PII: S0021-9290(99)00066-4

The relations between C_d and Re have been studied in detail for bodies with simple geometries for many years (Hoerner, 1965; McGoff, 1991) and the important role of hydrodynamic abilities during fish displacement has also been previously pointed out (Webb, 1975; Blake, 1983; Sagnes et al., 1997). It was revealed, for instance, that French freshwater fish species colonizing fast-flowing river areas showed a significant hydrodynamic adaptation (i.e., a lower C_d) compared to other species with slower-flowing preferences (Sagnes and Statzner, personal communication). Concerning human swimming, very few comparable studies were carried out. Clarys (1979) studied the different flowing conditions around a swimmer at swimming speeds going from 1.5 to $2\,m\,s^{-1}$; using a frontal surface area of the swimmer collected in a static position, he showed that the best consideration of this swimmer's C_d should be done at a Re of about $2\times10^5 - 2\times10^6$. Considering the great number of parameters occurring during swimming, the actual most pertinent method is the one developed by Hollander et al. (1986) (Measure of Active Drag or MAD MAX). It consists in measuring drag forces in "real" swimming conditions, as the swimmer bears his hands on submerged drag captors. Nevertheless, these studies remain rather general; they do not consider either the butterfly swimming style or the changes in body or limbs' positions (which induce changes in the frontal surface area of the body, and thus changes in drag).

The aim of this study is to define a new approach to determine the relationships between movements, hydrodynamics and performance of swimmers, and more particularly when they practice butterfly swimming. In this way, we have (i) determined the most propulsive positions during a submerged cycle in butterfly swimming; (ii) quantified the C_d at a given Re for each of these positions, by reproducing them on manikins, in order to determine the best hydrodynamic positions; (iii) compared, at a given Re, the hydrodynamic potentialities (i.e., the C_d) of two swimmers presenting different positions (and performances) during the same phase of a swimming cycle.

2. Material and methods

2.1. Kinematic study

Instantaneous measures of hip velocity were used to estimate swimming speed (Weigand et al., 1975) and to determine the most propulsive positions during the stroke. In this way, we had to collect the three-dimensional coordinates of swimmers' hip using a kinematic method. This study was carried out on the world's top-swimmers, who were filmed during the 100 m butterfly of the World Championships (Roma, 1994). We used two cameras (Sony EVO 150 TR, HI8, NTSC) with a frequency of 30 Hz, which was sufficient to study trajectories during an arm cycle (i.e., about 1 s). The cameras were placed in waterproof boxes (Sony SPK-TRA) which were securely fixed 0.6 m below the water surface. According to the requirements of the Fédération Internationale de Natation Amateure (FINA) and of the image analysis software developed by Schleihauf (1994), the waterproof boxes were fixed against the turning wall to ensure an angle of 90° between the respective optic axis of the two cameras (Fig. 1). Thus, each optic axis formed an angle of 45° with the displacement axis of the swimmers and the convergence of the optic fields allowed to study the swimmers of corridors nos. 4 and 5. Images were taken along a 12 m distance, beginning as swimmers reached the center of the pool (i.e., they had already swum 25 m). At the end of each image acquisition set, a 1.35 m long sighting mark was filmed in the central part of corridors 4 and 5; it was hereafter used as a scale to calibrate measurements obtained in the image analysis.

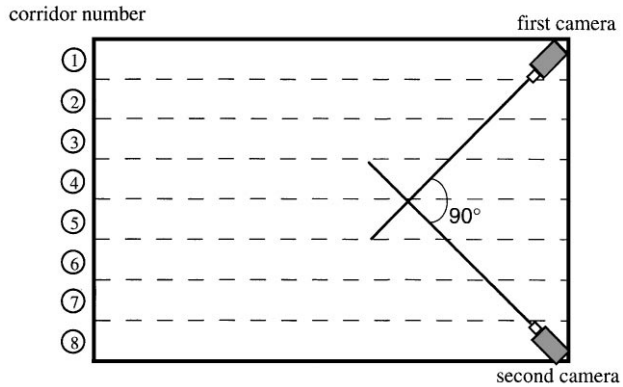

Fig. 1. Position of cameras used in a kinematic study of swimmers. Swimming corridor nos. 4 and 5 were used during the experimentation.

2.2. Video data treatment

The video views were digitized with a Targa board and stored in a PC computer. According to Schleihauf's kinematic analysis software (1994), the views were digitized frame by frame for one stroke (from the right blade entry to the same blade exit). For each frame, a background reference point (coordinates 0,0,0 in the reference system) and 22 points on the swimmer's body (including the hip position) were semi-manually digitized. Because of the 45° angle between each camcorder and the swimmer displacement during the data acquisition, the coordinates of each digitized point were rotated using a mathematical function. The trajectories of the points were obtained for each of the three dimensions: anterior — posterior (x), transversal (y) and vertical (z). As for all biomechanical data (Dainty and Norman, 1987), the trajectories were smoothed with a second-order polynomial function. Note that the reliability of the kinematic analysis system

(Schleihauf, 1994) has recently been supported by a comparative study on kinematic data obtained simultaneously with the kinematic analysis and the motion analysis system (Monteil et al., 1996). As the subjects did not present the same duration of a swimming cycle, the comparison of their movements was made possible by temporal normalization. For each subject, the total time of the swimming cycle was converted to 100% of time, and the position of the tip of the middle finger entry into the water was taken as the new spatial reference (coordinates (0,0,0)). For each digitized point, the coordinates (x, y, z) were calculated for each 5% of the total time of the swimming cycle using a linear interpolation.

2.3. Determination of the most propulsive positions during a butterfly swimming cycle

The swimming arm motions can be summarized by an entry, an external sweep, an inward sweep, a downward sweep and an upward sweeping movement (Taïar et al., 1999a) (Fig. 2). The lower limbs carry out a dolphin movement (i.e., an undulation) made up of a downward and an upward fluttering. Using the kinematic method, the comparison of the covered distance between two successive positions allowed to define the three most propulsive positions (i.e., the three positions before which the covered distance was the highest). These were: the end of the external sweep (beginning of the cycle), the end of the internal sweep (middle of the cycle) and the end of thrust (end of the cycle) (Fig. 2). Compared to swimmers presenting lower performances, the (ex) world champion (Denis Pankratov, from Russia) does not present the same instantaneous positions at these three moments of the cycle. Thus, in order to quantify the energy gain (or loss) induced by these different positions, we determined their C_d in different flow conditions (i.e., different Re). The three different key positions of the world champion and those of a swimmer presenting mean performances during these championships were reproduced on articulated manikins (Fig. 3) using the numerous body angles given by the image analysis software (Schleihauf, 1994). Drag measurements were then carried out on these six manikins.

2.4. Drag-measuring device and water channel

The drag-measuring device and its support were placed on an open water channel (Fig. 4). Manikins were fixed to the device by way of a 3 mm diameter stainless-steel rod, and the drag was measured through the deformation of four flexible parts (width = 0.2 mm). A strain gauge was fixed on each flexible part and the four gauges were connected as a Wheastone bridge. The latter was linked through a DIN plug (which minimized the resistance to microcurrents) to a conditioner equipped with a variable scale system (INFINITY C Gauges, INFC-S1). The conditioner displayed in real time the drag force (D) acting on the manikin. Its analog output was linked to a data acquisition card (ANA 12-T, Nautil©) which turned analog signals into digital signals, recognized by the computer (PC 486DX, 66 MHz). Finally, the software ANA 12LIB (Nautil©) was used to read the data. A custom made modification of this software was used to carry out the different mean calculations and statistical tests (see below), and displayed in real time the evolution of drag forces (which allowed a fast detection of any anomaly) during data collection.

The relation between drag values displayed by the conditioner and drag forces applied to the device was linear, and the calibration was done by hanging up masses of known weights to a cotton yarn horizontally fastened to the device through a block, for which friction was minimized. During all experiments, we did not measure values above 10^{-2} N to avoid damaging the flexible parts of the drag-measuring device.

Drag measurements were done in a water channel (length = 15 m; width = 25 cm; height = 40 cm) fed by a centrifugal pump. The maximal discharge in the channel was about 260 $m^3 h^{-1}$, and it was adjustable by a watergate. The water depth and an optimal flow stability were obtained by adjusting an upstream and a downstream gate.

2.5. Measurements and error evaluation

To avoid any deformation of the rod by the drag acting on the manikin, the submerged rod length was reduced to 5 cm. To estimate the rod drag, preliminary measurements were made on a 5 cm submerged rod alone at different current velocities. Then, the manikin drag was calculated as the difference between the manikin + rod system drag and the rod drag at the same velocity. Although this method has theoretical problems (the drag of the manikin + rod system is greater than the manikin drag summed with the rod drag, due to the interaction between the rod and the manikin, see Hoerner (1965)), results remained comparable because the different manikins were similarly conditioned.

For each manikin, drag was measured for 10 different current velocities. Water temperature (which allowed the calculation of water viscosity) was noted during the flow stabilization, which occurred within 5 min (for the lowest speeds) or less. Thereafter, flow velocity was measured using a propeller (Nixon Stream Flo with helix No 403) (see Fig. 4) at the place where the manikin head was positioned later. A mean velocity was calculated over 1 min, from six values.

Manikins were placed parallel to the main flow, in the water channel center, with the head at the depth where velocity was previously measured. Then, drag was measured after horizontally positioning the support of the device (verification with an air level). A mean drag was

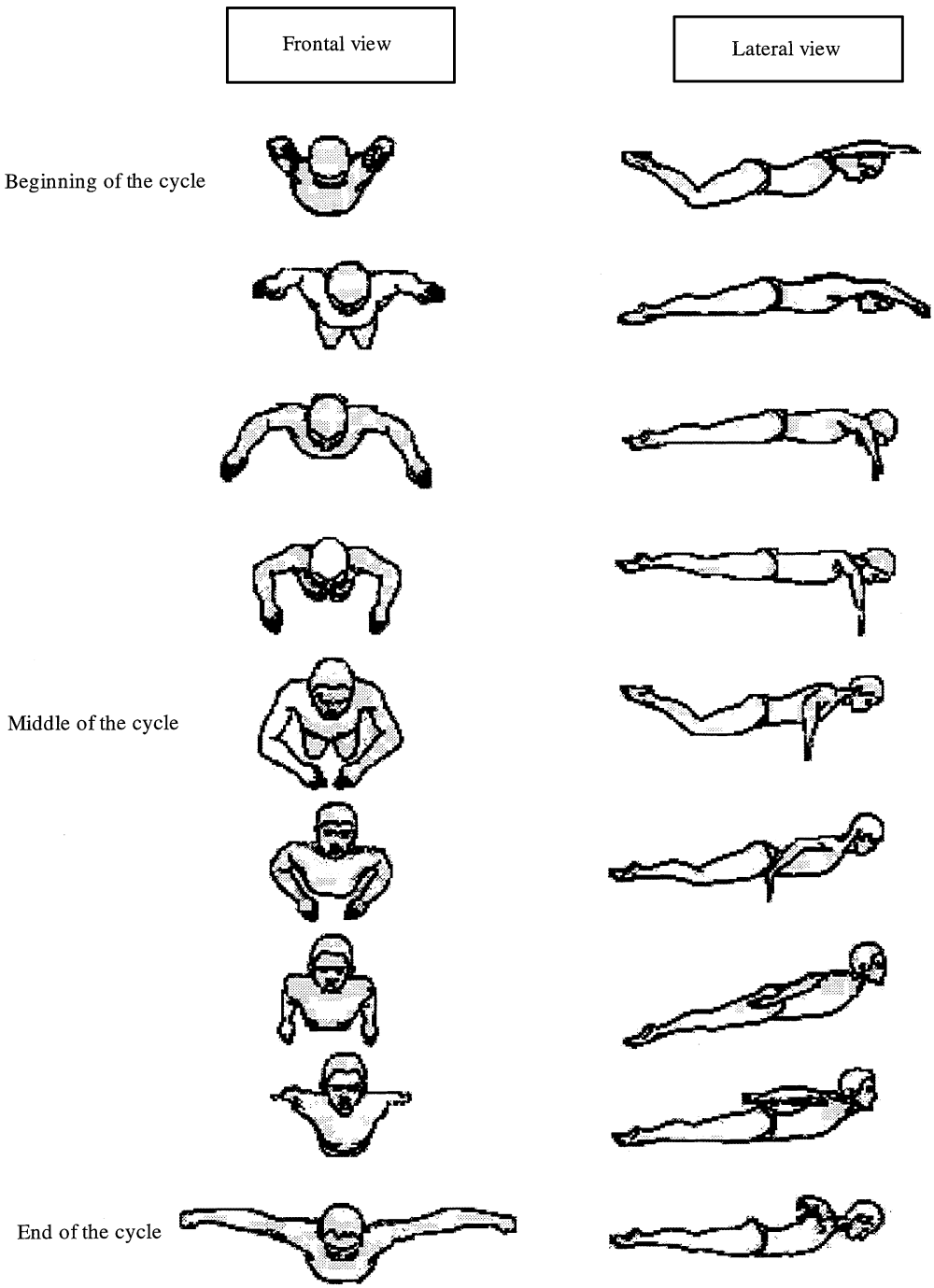

Fig. 2. Different phases of a butterfly swimming cycle.

calculated from 60 values collected over 1 min (95% confidence limits max = ± 5%), and the manikin was immediately removed from the water to avoid a deformation of the flexible parts of the device, which could occur if forces acted permanently.

Finally, the velocity was checked. If a Student *t*-test associated with an ANOVA confirmed the equality ($P < 0.05$) of velocity measurements before and after drag measurements, the subsequently used velocity would be the mean of these two values; if not, all the measurements would be repeated. When there were more than two values outside the 95% confidence limits (C_{95}) around the mean during one set of velocity or drag measurements, all measurements were repeated.

Then, the C_d values of manikins were calculated using Eq. (2), with S being measured using the image analysis

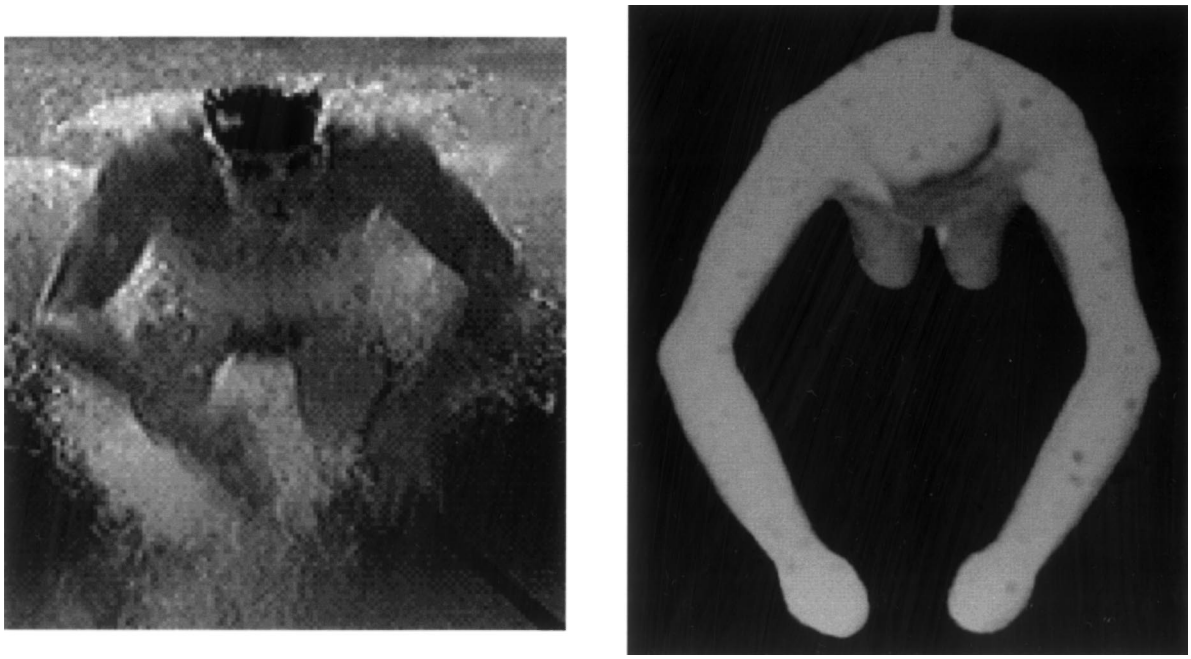

Fig. 3. Reproduction of a swimmer's position on a manikin (frontal view).

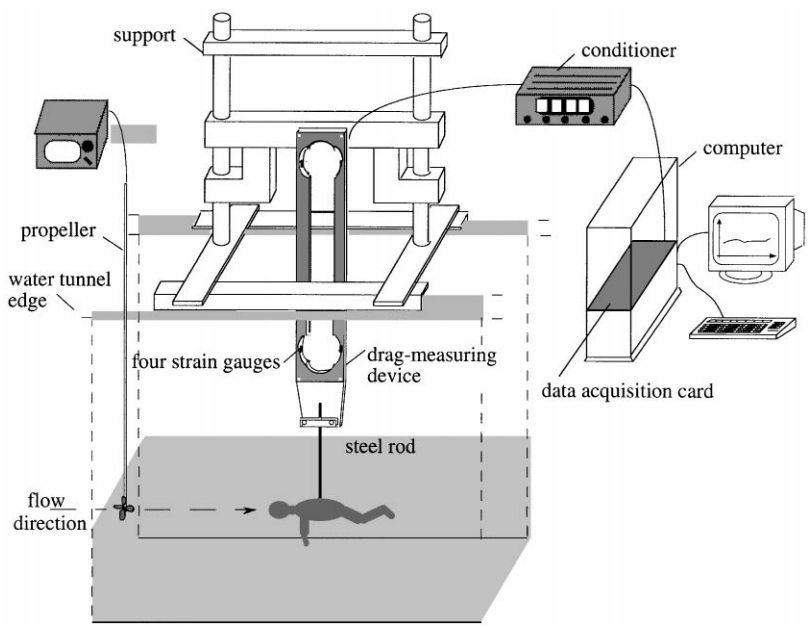

Fig. 4. Drag-measuring device used to determine drag forces on manikins, at known Reynolds numbers. Flow velocities were not simultaneously measured to do not perturb drag measurements.

method described by Taïar et al., 1999b. As all manikins' weights were similar, no more weight correction was necessary to ensure that the data were comparable.

Standard deviations on drag measurements (s.d.) were calculated using 30 repetitions of these measurements (30 means of each 60 individual measurements) on a manikin (external sweep position), at different current velocities. Repeatability was very good (Table 1) and we found that s.d. of drag values were closely related to the flow conditions, following the formula (C_{95} of the estimated parameter in brackets):

$$\text{s.d.} = 5.877 \times 10^{-12}(\pm 0.988 \times 10^{-12})\text{Re}^2 + 0.010 \qquad (4)$$

Table 1
Mean drag (D_m) and standard deviation (in brackets) from 30 drag measurements on a manikin (external sweep position), at different Reynolds numbers relative to the total length of the manikin (Re)

Re	$D_m(N)$
2.02×10^4	0.021 ($\pm$ 0.0035)
2.54×10^4	0.023 ($\pm$ 0.0036)
2.91×10^4	0.033 ($\pm$ 0.0010)
3.39×10^4	0.037 ($\pm$ 0.0010)
4.08×10^4	0.046 ($\pm$ 0.0010)
4.26×10^4	0.050 ($\pm$ 0.0010)
4.87×10^4	0.060 ($\pm$ 0.0010)
5.36×10^4	0.087 ($\pm$ 0.0030)
5.91×10^4	0.087 ($\pm$ 0.0020)
6.52×10^4	0.095 ($\pm$ 0.0020)

($n = 30$; $r^2 = 0.96$, $P < 0.001$).We applied this formula to calculate C_{95} for all values of all the manikins.

2.6. Hydrodynamic comparisons between different swimming positions

For a given phase of the swimming cycle (i.e., beginning, middle and end of the cycle) and at a given Re, an ANOVA I was carried out to see whether there were significant differences ($P < 0.05$) between the C_d of the "Pankratov" manikin and that of the other manikin. In the affirmative case, the observed differences should be explained by the different positions assumed by the different swimmers.

3. Results

For the first studied position (external sweep at the beginning of the swimming cycle, Fig. 5a), at low Re (from 2.5×10^4 to 4.0×10^4), C_d rapidly decreased in both manikins from a value of about 1.8 to about 0.9. At higher Re (from 4.0×10^4 to about 8.0×10^4), C_d values changed towards a threshold value of about 0.8. In all this Re range, there were no significant differences between the C_d values of the two manikins.

For the second studied position (internal sweep at the middle of the swimming cycle, Fig. 5b), the obtained C_d values were higher (from about 2.5 at an Re of 2.0×10^4 to the threshold value of about 1.0 for the highest Re) than those obtained for the previous position. The effect of the swimmer's position during this phase of the cycle was observed only at the lowest Re values: C_d values of the world champion were lower than those of the other swimmer for an Re range of $2.0 \times 10^4 - 3.5 \times 10^4$. There were no significant differences between the C_d values of the two manikins for Re above 3.5×10^4.

In opposition to the two previous positions, the curve obtained for the last studied position (thrust at the end of the swimming cycle, Fig. 5c) did not show any breaking-down point; the curve was exponential and C_d values progressively decreased from about 1.8 to 0.7 as Re values increased. The stabilization of C_d values occurred for higher Re ($> 6.0 \times 10^4$) than during the two previous experiments. Whatever the studied Re range, all the C_d values of the manikin of the world champion were significantly lower than those of the other manikin.

4. Discussion

The determination of manikins' positions from a dynamic study of swimmers better traduces the real swimming conditions (e.g., different frontal surface areas with respect to the swimming position) than static anthropometric considerations such as those of Clarys (1979). When compared to the MAD MAX method of Hollander et al. (1986), the strength of this study is to consider real swimming movements (e.g., the hand incidence is biased in MAD MAX as it acts on a solid support); however, our method does not allow one to collect drag values in a dynamic way during an entire swimming cycle.

The curves representing the obtained C_d values with respect to Re values were consistent with the theory of fluid mechanics; whatever the phase of the swimming cycle, C_d values decreased and then reached a threshold value for the highest Re values. Due to the little size of our manikins, we worked at lower Re values than those encountered by real swimmers (i.e., of about 3.6×10^6 for a swimmer of height 180 cm and swimming at 200 cm s^{-1}). Nevertheless, as we approached the threshold value of C_d at our highest Re values, we could expect that the theoretical decrease in C_d values at higher Re should be reduced, and that the following discussion should remain unchanged in real swimming conditions.

In wings, C_d values do not become stable until Re reaches 9.0×10^6 (Hoerner, 1965). The stabilization of the C_d values of our manikins at lower Re values (9.0×10^4, Fig. 5) could be due to several factors. First, the water flow in the channel was already turbulent and the calculated Re values were under-estimated. Second, although the manikins presented a smooth surface texture, their limbs' positions should induce a turbulent flow around the body (i.e., a stabilization of C_d values) at low Re values.

For the same swimmer and at comparable Re values, C_d values changed according to the phase of the swimming cycle; they were important during the middle part of the cycle (Fig. 5b) and reduced at the beginning (Fig. 5a) and at the end (Fig. 5c) of the cycle. As expected, drag was smaller during the less propulsive phases of the swimming cycle, and the swimmer should take advantage of these phases to take up a hydrodynamic position. In this case, upper and lower limbs are in the continuation of the trunk and the body is relatively streamlined.

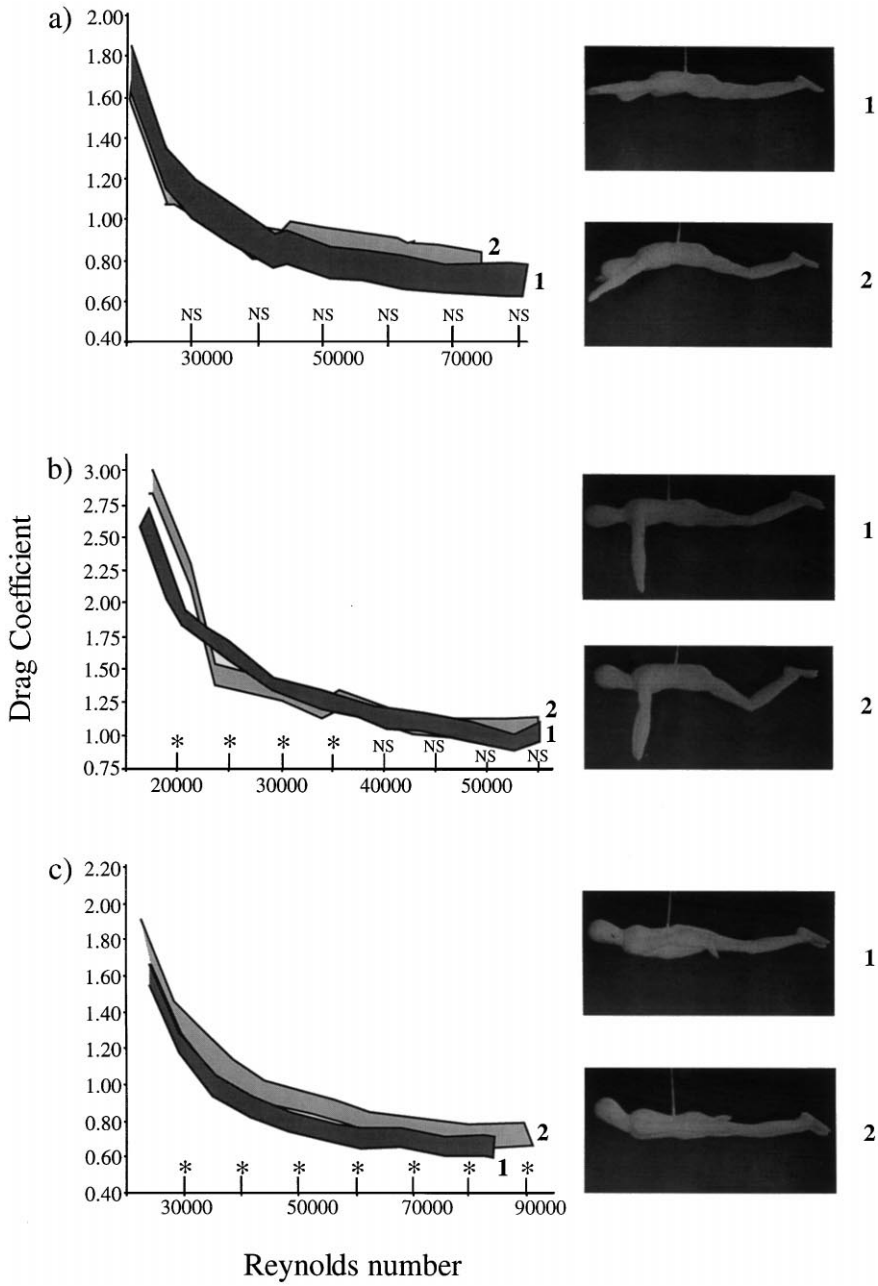

Fig. 5. Drag coefficient against Reynolds number for manikins representing swimmers in different positions during three phases of a butterfly swimming cycle. (a) Beginning of the cycle; (b) middle of the cycle; (c) end of the cycle. Manikin 1 represented the ex-world champion (Pankratov) and manikin 2 another swimmer. At a given Reynolds number, the difference between the curves was significant (*) or not (NS).

During the middle of the swimming cycle, the upper limbs are in a vertical plan, perpendicularly to the swimmer's displacement (i.e., perpendicular to flow) which induces a high C_d due to the increase of the frontal surface area (see Eq. (2)). However, note that our drag measurements during the middle part of the cycle (Fig. 5b) are biased by the static condition of manikins. In real swimming conditions, during this phase of the cycle, the arms are moving, the relative speed between them and the water decreases and thus the hands and forearms do not contribute to active drag at all. As a result, we can expect that our method overestimates C_d values at mid-stroke, and future studies should consider separately the drag produced by limbs' movements.

At comparable Re values and for a given phase of the swimming cycle, C_d values depend on the position of the swimmer. When significant differences were observed between the two swimmers studied, Pankratov was always presenting the lowest C_d values. Even during the less propulsive phases of the swimming cycle (i.e., beginning

and end of the cycle), the world champion was more streamlined than the other swimmer. The legs of the latter were more bent and his arms less stretched at the beginning of the cycle (Fig. 5a), whereas his head was more raised at the end of the cycle (Fig. 5c); this should increase his C_d by increasing his frontal surface area. Obviously, the frontal surface area is not the only parameter that should be considered to explain performance, but the ex-world champion exploit could certainly be correlated with his faculty to adapt his frontal surface area in a way to minimize drag during the main phases of the swimming cycle.

5. Conclusion

It is obvious that the "choice" of swimming movements in a way to reach a maximal swimming speed depends as much on their propulsive faculties as on their abilities to minimize drag. The tools and methods described in this study allow to quantify drag and our results showed that the fastest swimmers seem to optimize the ratio between thrust and drag by adapting their movements during a few phases of the swimming cycle. Future studies should focus on making experiments in "real" swimming conditions (i.e., at higher Re values), which could allow to understand better how to minimize drag (and thus reduce energy losses due to non-optimal movements) during swimming.

Acknowledgements

Cécile Polo is gratefully acknowledged for linguistic advices.

References

Blake, R.W., 1983. Fish Locomotion. University Press, Cambridge, pp. 208.

Clarys, J.P., 1979. Human morphology and hydrodynamics. In: Terauds, J., Bedinfield, E.W. (Eds.), International Series on Sport Sciences Swimming III. University Park Press, Baltimore.

Dainty, D.A., Norman, R.W., 1987. Standardizing Biomechanical Testing in Sport. Human Kinetics, Champaign, IL.

Hoerner, S.F., 1965. Résistance à l'Avancement dans les Fluides.. Gauthier Villars, Paris, pp. 471.

Hollander, A.P., Groot, G.de, Ingen Schenau, G.J.van, Toussaint, H.M., Best, H.de, Peeters, W., Meulemans, A., Schreurs, A.W., 1986. Measurement of active drag during crawl arm and stroke swimming. Journal of Sport Science 4, 21–30.

McGoff, H.J., 1991. The hydrodynamics of conodont elements. Lethaia 24, 235–247.

Monteil, K.A., Chèze, L., Masset, J.B., Rouard, A.H., 1996. Three dimensional analysis of the human gait: comparison between the motion analysis and the kinematic analysis systems. In Proceedings of the Fourth International Symposium on 3-D Analysis of Human Movement. University of Joseph Fourier Grenoble 1, France, pp. 49–52.

Sagnes, P., Gaudin, P., Statzner, B., 1997. Shifts in morphometrics and their relation to hydrodynamic potential and habitat use during grayling ontogenesis. Journal of Fish Biology 50, 846–858.

Schleihauf, R.E., 1994. Kinematic analysis software for three dimensional data handbook. (KA Software, Version 4.0).

Taïar, R., Sagnes, P., Rouard, A.H., 1999a. Modification of the frontal surface area during butterfly swimming.

Taïar, R., Sagnes, P., Rouard, A.H., 1999b. Image digitalization as a new method to determine anthropometric parameters and surface area on swimmers.

Vogel, S., 1994. Life in Moving Fluids. second ed.. Princeton University Press, Princeton, pp. 467.

Webb, P.W., 1975. Hydrodynamics and energetics of fish propulsion. Bulletin of Fisheries Research Board of Canada 190, 1–160.

Weigand, K., Wuensch, D., Jaehnig, W., 1975. The division of swimming strokes into phases based upon kinematic parameters. In: Clarys, J.P., Lewillie, L. (Eds.), Swimming, 2. University Park Press, Baltimore.